Acta Geotechnica (2023) 18:1391–1405
https://doi.org/10.1007/s11440-022-01675-6

RESEARCH PAPER

Interpretation of field tests using geo-statistics and Kriging to assess the deep vibratory compaction of the Dike A21, Diavik Diamond Mine

Joshua Schorr[1] · Roberto Cudmani[1] · Konrad Nübel[2]

Received: 8 February 2022 / Accepted: 9 August 2022 / Published online: 2 September 2022

Abstract
This article presents an interpretation and statistical analysis of heavy dynamic probing (DPH) tests carried out on the compacted core of Dike A21, of the Diavik Diamond Mine. Due to the inhomogeneous and inherently random nature of soil and the uncertainties associated with even well controlled field tests such as DPH tests, the evaluation of in situ properties (such as density) should take into consideration the natural variability of the soil. Aided by the large amount of relatively concentrated field data, this paper presents a methodology for not only evaluating the field tests statistically through Kriging, but also for judging the compaction effort, taking into consideration the variability. This paper documents the necessary normalization procedure, analyzing a number of external factors such as the temperature, time since compaction (aging) and the presence of nearby works that may affect the field data. It was shown that the appraisal of soil improvement measures should consider the presence of natural and unavoidable fluctuations of the fill material. The Kriging estimate combined with an averaging procedure and subsequent comparison with the expected variability, quantified by the variogram, was applied which enabled the assessment of areas with insufficient compaction. Additionally, the influence of aging of the fill was demonstrated, where a clear increase in the DPH tests between 0 and 14 days since compaction was observed. It was also found that over-compaction leads typically to a lower relative density. The authors note that this statistical analysis was performed following the control and acceptance of the compaction of the dike and as such had no impact on the acceptance of the dike construction.

Keywords Aging · Data analysis · DPH · Field testing · Kriging · Statistical evaluation

1 Introduction

The inherent variability of soil has been widely documented in the literature, particularly within the realm of field testing, where even homogenous soil layer can often show significant variation (e.g., [4, 19, 31, 37, 40]). Even in improved soils, significant variations in the results of field tests have been observed (e.g., [1, 35]). In the construction industry, the treatment of areas subjected to soil improvements, which have been identified as not meeting a certain conformance criteria through field testing or other testing means can be ambiguously described in the relevant contract documents, e.g., a target value is specified, but the relationship for the interpretation of the target quantity is not. With regard to soil improvement, it is important that a differentiation is made between insufficient compaction and the effects of soil variability. The application of

✉ Joshua Schorr
joshua.schorr@tum.de

Roberto Cudmani
roberto.cudmani@tum.de

Konrad Nübel
konrad.nuebel@tum.de

[1] School of Engineering and Design, Institute of Soil Mechanics, Foundation Engineering, Rock Mechanics and Tunnelling, Technical University Munich, Franz-Langinger Street 10, 81245 Munich, Germany

[2] School of Engineering and Design, Chair of Construction Process Management, Technical University Munich, Arcistraße 21, 80333 Munich, Germany

methods of geostatistical analysis affords an opportunity to assist in making such a judgment.

The following study is based on an analysis of field testing with the heavy dynamic probe (DPH), tests which were carried out within the inner core of a section between Stations 0+983 and 1+366 of the Dike A21, a part of the Diavik Diamond Mine. The location of Dike A21, a plan view with chainages, as well as a typical cross-section can be seen in Fig. 1 and Fig. 2. The goal of this article was to assess the success of the vibro-compaction effort based on state of the art statistical methods. To evaluate the relative density from the DPH tests, an interpretation method based on the cavity expansion theory and calibration parameters from a similar soil was used.

In total, the results of 201 DPH tests were made available between Station 0+983 and 1+366, of which 45 tests were excluded due to incompleteness of the data. For each of the tests, the following information was made available:

- Number of blow counts per 10 cm penetration;
- Date since compaction;
- Location of the test—corresponding to a northing and easting;
- A bucket count number, which describes the additional fill material dumped into the hole resulting from the dynamic testing; and
- Aditional information regarding vibratory compaction works being carried out in the vicinity.

This well-documented and large dataset corresponded to an area of approximately 20 m^2 per DPH (based on a 10-m-wide inner core zone) test and is ideally suited to stochastic analysis, a field of science which was pioneered by Vanmarcke [39], and has been gaining significant attention in recent times (e.g., [30] or [28]).

The use of dynamic probing to assess the in situ density of soils has long been established in the geotechnical community, e.g., Melzer [24] demonstrated its use in sand, Biedermann [2] in silt, and Butcher et al. [5] demonstrated its applicability to the interpretation of clay soils. The European Standards, EN 1997-2:2007 and EN 22476-2:2012 allow for the use of such methods for the assessment of the strength and deformation properties of soil, primarily for non-cohesive soils, but also under certain circumstances it allows for its use in the interpretation of cohesive soils. EN 1997-2:2007 provides empirical relationships between the dynamic probing results and the density index, however, these relationships do not account for the mean pressure, which strongly influences the penetration resistance, and thus must be used with caution.

One common limitation of penetration tests such as the cone penetration test (CPT), standard penetration test (SPT) and the dynamic probing (DP) in coarse-grained soils is related to the grain size and more specifically to the ratio between the mean grain size D_{50} and the diameter of the tip of the probe d_p. In the case of the CPT, it is generally accepted that the influence of the single grain on the penetration resistance can be disregarded for a ratio d_p/D_{50} of about 10 to 20 (e.g., [3, 21, 33]). It is however to be noted that recent simulations with the discrete element method (DEM) by Khosravi et al. [17] report an increase in the calculated tip resistance of only 10% for a d_p/D_{50} ratio of 2.1 compared to the baseline of 3.1 (with however, a 100% increase in the standard deviation, indicating a greater fluctuation), a finding that shows a reasonable agreement with the 20% increase in cone penetration resistances recorded by Bolton et al. [3] for Leighton Buzzard Sand. As far as the authors are aware, little research has been carried out into the dependence of the penetration resistance of dynamic probing in sandy gravels with D_{50} around 2–10 mm as present in Dike A21 (e.g., Melzer [24] examined sands with a maximum D_{50} of 4 mm and Biedermann [2] does not provided relationships for gravels). A newer study investigating the correlation between CPT and DPH results by Mahler and Szendefy [22] (who investigated soils with a D_{50} of up to 10 mm) suggests that such correlations can be applied up to $d_p / D_{50} \approx 5$, with a larger scattering being observed for $D_{50} > 2$ mm. Furthermore, the work by Karray and Hussien [16] which synthesized a number of studies comparing the cone penetration resistance obtained from the CPT with shear wave velocities indicates an increase in the fluctuation with increasing mean grain size.

According to Ghafghazi et al. [12] the Becker penetration test (BPT) is more suitable than other field testing tools in the characterization of coarse soils due to the significantly larger probe diameter of 168 mm, compared to the DPH with a diameter of 50 mm, thus reducing single grain effects on the dynamic penetration resistance. For this reason and also because experience with the compaction control of previous neighboring and comparable dikes was available, acceptance criteria in the Diavik project were based on BPT results, which ultimately provided the confidence on the compaction of the core of Dike A21. Nevertheless, since the purpose of this contribution is to develop a geostatistical procedure to evaluate the success of deep compaction, it is assumed that the penetration resistance of the dynamic probing correlates with the density of the soils in the dike. Based on the experimental investigations of Melzer [24], who found out that the influence of the rod friction on penetration in granular materials can be disregarded for sounding depths less than around 10 m (the average height of the compacted core was 12 m) it is assumed for this study that the rod friction is negligible.

1.1 Site description

The A21 dike and the neighboring dikes A418 and A154 are located within the Lac de Gras, situated approximately 220 km south of the Arctic circle and 300 km north of Yellowknife, in Canada's Northwest Territories and were constructed to facilitate dewatering and the subsequent open pit extraction of diamonds.

Located within the arctic climate region, the temperatures (daily average) at the Lac de Gras range from − 32 °C in winter to + 15 °C in summer. These extremely low temperatures could account for the very high penetration resistance encountered in the upper layers of the dike fill and meant that boring had to be undertaken before DPH tests could be carried out in some areas. It is noted that that permafrost is present within the shallower regions of the lake, corresponding to approximately Sta. 0+450 m (Fig. 2). The geology at the A21 site consists predominantly of a thin layer of highly compressible silt with low plasticity clay, followed by a non-plastic glacial till and a bedrock of tonalite and quartz diorite.

The cross section of the dike, depicted in Fig. 2b, was constructed out of waste rock from a nearby stockpile consisting of an outer zone of primary and secondary crushed material (Zone 3 and Zone 2, respectively) with grain sizes of 10–1000 mm and an inner zone from tertiary crushing (Zone 1), consisting of sandy gravel with grain sizes between 0.1 and 50 mm with a fine content of < 10% (see Fig. 2 c).

To prevent water seepage through the dike from the upstream side, a cutoff wall consisting of low strength plastic concrete was to be installed. To reduce the expected vertical and horizontal deformations of the dike, facilitate the construction of the cutoff wall, as well as to reduce the axial and bending forces on the wall and thus the extreme fiber stress through the expected negative skin friction as a result of the fill settling greater than the concrete following the dewatering, the supporting approximately 10-m-wide core area of the dike was to be compacted with the vibro flotation technique (see e.g., [34]). The planned depth of the treatment varied between 5 m and 22.5 m with an average depth of approx. 12 m. The DPH tests were carried out exclusively in the compacted inner core area.

1.2 Interpretation of the DPH tests

For the analysis it is assumed that a successful vibro-compaction of the inner core zone corresponds to a dense state and a relative density of 70%, with the success of the vibro-compaction being assessed by the results of DPH tests based on an estimation of the relative density from the number of blow counts for 10 cm of penetration, N_{10}.

Several interpretation models for DPH test results can be found in the literature, one of which is the empirical correlation from Kralik [18] between the cone penetration resistance, q_c (in MPa), and the number of blow counts for 20 cm penetration, N_{20}, which simplifies to:

$$q_c = 1.095 + 0.476N_{20} \approx 0.5 \cdot N_{20} \approx N_{10} \quad (1)$$

Fig. 1 Location of the Diavik Diamond Mine adapted from [41]

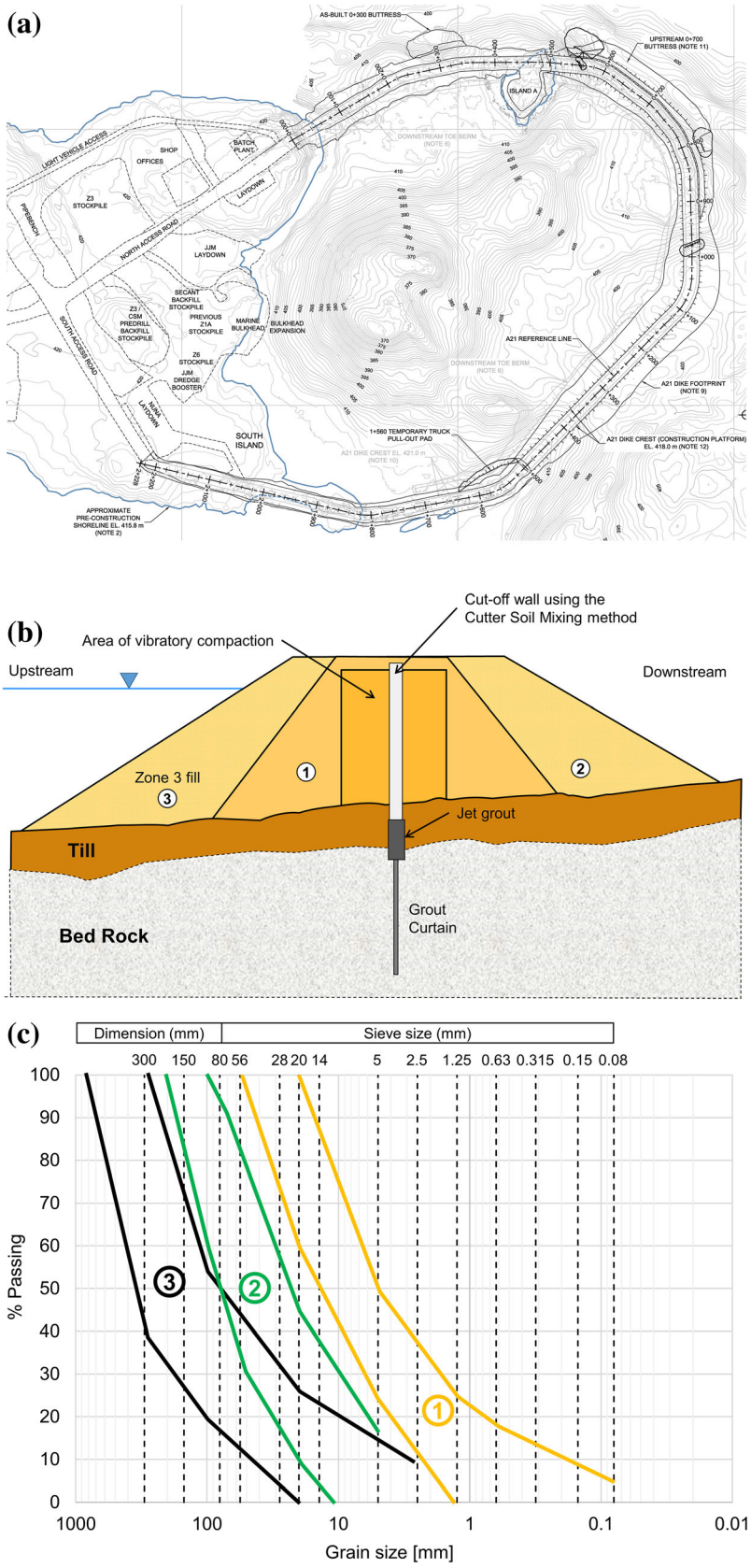

Fig. 2 **a** Plan view of the dike, **b** schematic representation of the dike core including the area to be vibro-compacted and **c** grain size distribution limits for the fill material

Mahler and Szendefy [22] proposed a relationship based on a normalized CPT-DPH ratio, taking into consideration the mean grain size and the vertical stress, with after considering an average grain size of the inner core of 10 mm, treatment depth of 12 m and buoyant unit weight of $\gamma' = 10.6\,\mathrm{kN/m^3}$ the following relationship can be obtained:

$$q_c\,(\mathrm{MPa}) = 1.51 \cdot N_{20} \tag{2}$$

meaning that the relationship by Kralik [18] is conservative, corresponding to an average grain size of approximately 0.3 mm. For the statistical analysis, the more conservative relationship from Kralik [18] was used for the estimation of the q_c as it was deemed to be more representative.

The relative density, D_R (in %), can be estimated based on the cone penetration resistance q_c as a function of the vertical effective overburden stress σ'_{v0} by Jamiolkowski et al. [15] with

$$D_R = -98 + 66 \cdot \log_{10}\left(\frac{q_c}{\sqrt{\sigma'_{v0}}}\right) \tag{3}$$

for young, normally consolidated, quartz-based sands derived from calibration chamber tests.

However, in a subsequent publication the correlation from Jamiolkowski et al. [14] was modified to take into account the effect of the calibration chamber boundaries on q_c resulting in

$$q_c = 205 \cdot e^{2.92 \cdot D_R} p'^{0.51} \tag{4}$$

where p' is the mean effective stress and along with q_c can be calculated in kPa. Assuming an effective peak frictional angle of φ' of 42° based on site investigations for the densified fill from the stress deformation analysis of the dike, p' can be calculated from the well-known relationship $K_{NC} = 1 - \sin\varphi'$ [13] leading to $p' \approx 1.66\sigma'_v/3$. However, to allow for the effects of compaction, for the subsequent statistical analysis a conservative estimate of $K_0 = 0.5$ was selected, leading to $p' \approx 2\sigma'_v/3$ and thus a lower estimation of the relative density. Using the conservative estimate of K_0 this modification caused a reduction in the estimated q_c of approximately 20%.

According to Cudmani [9] the following semi-empirical relationship can be used to estimate the density index:

$$q_c = k_q \cdot p_{LS} \tag{5}$$

where the empirical shape factor (for granular soils) k_q, and the limit pressure p_{LS}, obtained through the expansion of a spherical cavity in a corresponding granular material that considers properties such as the grain shape and the grain hardness, are both dependent on the density index I_D. The shape factor can be calculated using the empirical relationship

$$k_q = 1.5 + \frac{5.8 \cdot I_D^2}{I_D^2 + 0.11} \tag{6}$$

and the limit pressure with

$$p_{LS} = \left(a_1 + \frac{a_2}{a_3 + I_D}\right) \cdot p'^{b_1 + \frac{b_2}{b_3 + I_D}} \tag{7}$$

where a_i and b_i are material constants calculated by numerical simulations of the spherical cavity expansion using the hypoplastic model (see [9]), independent of I_D and p'. For the interpretation of the DPH tests, material constants corresponding to Ticino sand were selected, a poorly graded quartz river sand (SP) according to the unified soil classification (see [9]). For Ticino sand the material constants are: a_1=3.055, a_2=−6.686, a_3=−1.255, b_1=0.794, b_2=0.133 and b_3=−1.379.

Thus, the cone penetration resistance was first determined from the DPH tests based on Eq. (1), after which the density index of the fill material was calculated as the solution to Eq. (5), (6) and (7). Though not completely representative of the fill material in the inner core—Ticino sand typically does not have any significant gravel component—it was chosen for use in this study due to the lack of experimental data for material calibration of the used fill material. According to Cudmani [9] however, no relationship was found between q_c and the mean grain size, rather on the grain hardness and the grain shape.

1.3 Comparison of the DPH results

The required number of blow counts per 10 cm to achieve an assumed target relative density D_R of 70% according to the relationship proposed by Jamiolkowski et al. [14, 15] and Cudmani [9] is compared in Fig. 3 with the blow counts from the DPH tests average blow count per depth increment $\overline{N}_{10}$, the bounds $\overline{N}_{10} \pm s_{N_{10}}$, where $s_{N_{10}}$ is the standard deviation. Here, the interpretation models are also compared with the average and lower bound of the results of the DPH testing on previously completed dikes A154 and A418 several years following the construction of the dikes, labelled Criteria in Fig. 3.

This comparison reveals several conclusions. Firstly, if only the average blow count for all of the DPH tests is considered, the criteria of $D_R > 70\%$ has been fulfilled—both according to the interpretation models and according to experience from the neighboring dikes. Secondly, it would appear that the recorded blow counts from the DPH tests at dike A21 do not appear to show a sharp increase after approximately 14 m, as per the DPH tests at neighboring dikes A154 and A418. One possible cause for this

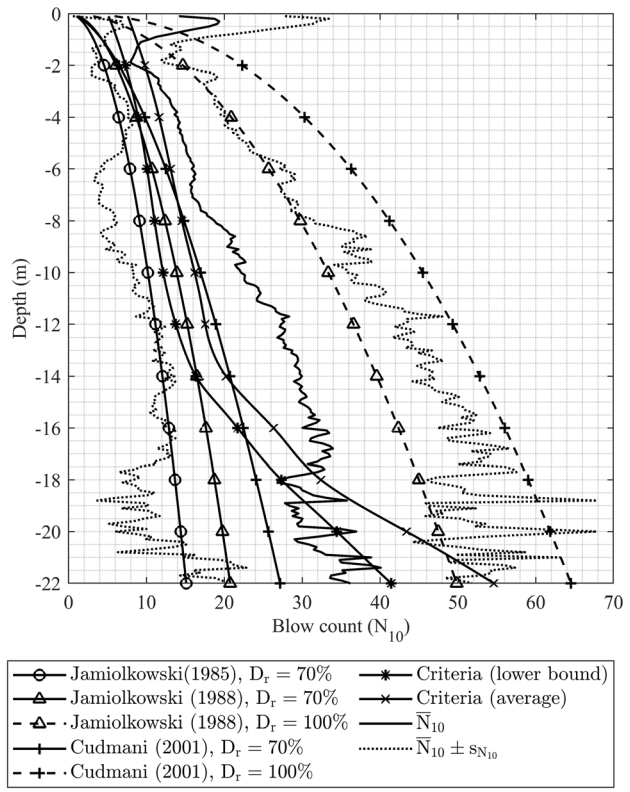

Fig. 3 Comparison of the average blow count per depth with the project criteria and various methods for evaluating the density index

difference is that the DPH tests were undertaken at dike A418 approximately 10 years after construction. It could be conjectured that the sharp increase in the recorded blow count be attributed to either 'aging' of the fill material, a well-documented phenomena—even in granular material (e.g., [26]), or to an increase of the shear strength of the material due to a decrease in the temperature (e.g., [20]). Thirdly, assuming an average compaction of $> 70\%$ (based on the assumption that the compaction procedure was approved), comparison of the actual blow counts shows a greater agreement with the required blow counts with the methods according to Jamiolkowski et al. [14] and Cudmani [9]. These models, along with Jamiolkowski et al. [15], involve a logarithmic increase in the recorded blow counts with the depth (or overburden stress). It should be noted that despite a homogenous fill material and a consistent method of compaction, inspection of $\overline{N}_{10} \pm s_{N_{10}}$ both reveals a very high degree of fluctuation. Due to the fact that the upper bound of the recorded blow counts $\overline{N}_{10} + s_{N_{10}}$ lies above the theoretical attainable relative density according to Jamiolkowski et al. [14], the relationship proposed by Cudmani [9] appears to provide a better framework for interpreting the DPH data.

1.4 Stochastic analysis

Uzielli et al. [37] describe the practical modeling of the soil variability in terms of a geotechnical property as a random field based on the results of cone penetration tests with the following relationship:

$$Z(s) = t(s) + w(s) \tag{8}$$

where $t(s)$ is a deterministic trend function, $w(s)$ is a fluctuating component, $Z(s)$ is the in situ soil property, and s is a spatial position (e.g., the vertical direction for this example of DPH testing). This approach will be followed in the analysis of the DPH tests by first de-trending the data through a normalization procedure.

1.5 Normalization of the DPH test results

The relative densities were determined at all data points through the interpretation relationships proposed by Jamiolkowski et al. [14] and Cudmani [9], using Eq. (1) and the inverse solution to Eqs. (5)–(7). In Fig. 4, the average of the achieved density index per depth increment is compared with the project requirement and the number of conforming tests is displayed (right). As can be seen from the figure, the criteria of $I_D \geq 0.7$ ($D_r \geq 70\%$) are generally met by the average achieved density, for both interpretation methods. The average density indexes achieved according to Cudmani [9] show some areas below the criteria, e.g., at depths 6–8 m and 17–20 m; however, in Jamiolkowski et al. [14] all averages were above. This can be explained by the fact that the density index of the average blow counts is not equal to the average of the density index calculated from the individual blow counts due to the nonlinear relationship. Furthermore, the interpretation according to Cudmani [9] appears to be more conservative than that of Jamiolkowski et al. [14] with average density indexes being recorded of 0.75 and 0.85, respectively.

Without direct measurements of the actual density, it is impossible to judge from Fig. 4 which interpretation method provides the most accurate evaluation of the density index in the core of the dyke. However, under the assumption that a homogenous compaction of the fill material was achieved, including down to the base of the fill, a constant density index would be expected. The results of the normalization seem to confirm this, as aside from in the upper 5 m and lower 5 m, a relatively constant relationship of the density with the height can be seen. It can be conjectured that the higher values at the surface are caused by a combination of the additional compaction due to the construction traffic and the freezing of the upper soil layers in the winter months. The large variations in the lower depths are attributed to the small number of conforming records, which can be seen in the right of the figure, and the

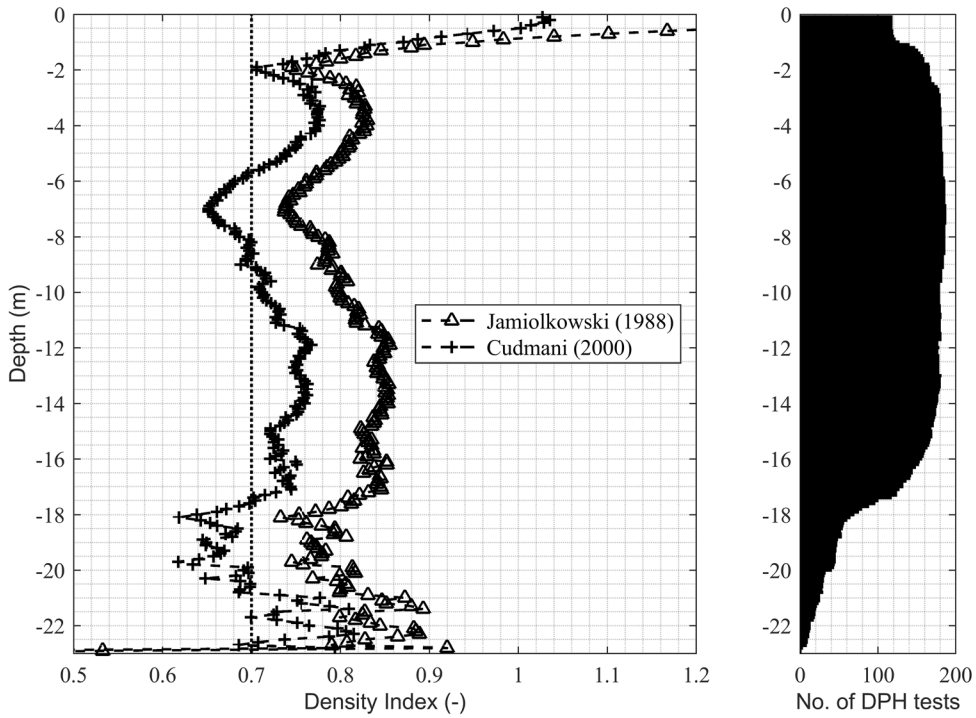

Fig. 4 Estimated density index according to Jamiolkowski et al. [14] and Cudmani [9] compared with the required density index of 0.7 (left), and the number of conforming DPH tests at each depth increment (right)

effectiveness of the vibro-compaction method. Based on this assessment, only results between 5 m and 20 m have been considered in the further statistical analysis.

Part of the DPH documentation included recording:

1. The number of days since compaction was carried out at the compaction point(s) adjacent to the DPH tests;
2. Whether or not additional vibro-compaction was carried out since at other locations within the vicinity (50 m); and
3. Whether or not vibro-compaction within the vicinity (50 m) was being carried out during the DPH testing.

Additionally for each vibro-compaction location, the following was made available:

4. The number of loader bucket counts filled during the compaction process.

The effect of "aging" of the granular fill—quantified by an increase in the density index over time, following placement or dynamic compaction—has been well documented in the literature (e.g., [6, 25, 27, 34]). The physio-chemical causes for this phenomenon are not the focus of this article, rather the influence of this phenomenon—which is explored in Fig. 5b, where the average number of blow counts over the depth corresponding to: 1–7 days, 8–14 days, 15–21 days and more than 21 days since vibro-compaction at the compaction point adjacent to the test was carried out, and in Fig. 5c where the distribution of the estimated density index was plotted as a boxplot (± 25% quantiles, median, maximum and minimum limits as well as outliers) over the time since compaction. Analysis of the data in Fig. 5b shows a large increase in the number of recorded blow counts per 10 cm between tests carried out < 7 days compared to tests carried out between 15 and 21 days following compaction; however, this increase is significantly less pronounced when compared with the results of the tests carried out after 21 days. This is confirmed in Fig. 5c where a pronounced increase in the density index can be observed within the first 14 days, both in terms of the median value and the ± 25% quantiles. From approximately 21 days, the density index appears to decrease slightly and a significantly higher variance can be observed, evidenced by the scattering of the medians, possibly due to a reduction in the data points or to other unkown factors. The time dependence can also be assessed based on the relationship of the normalized (vertical stress) tip resistance proposed by Charlie et al. [6], however, this relationship was not found to be able to explain the increase of the density index within the first two weeks. For further analysis, only results of DPH tests conducted 14 days or more after compaction were considered.

The influence of vibro-compaction within 50 m of the DPH tests, both prior to the test and during the test, is analyzed in Fig. 5a. Here it is evident that the vibro-compaction conducted concurrently to DPH testing results in a lower number of recorded blow counts, probably caused by excess pore-water pressures and the large vibrations

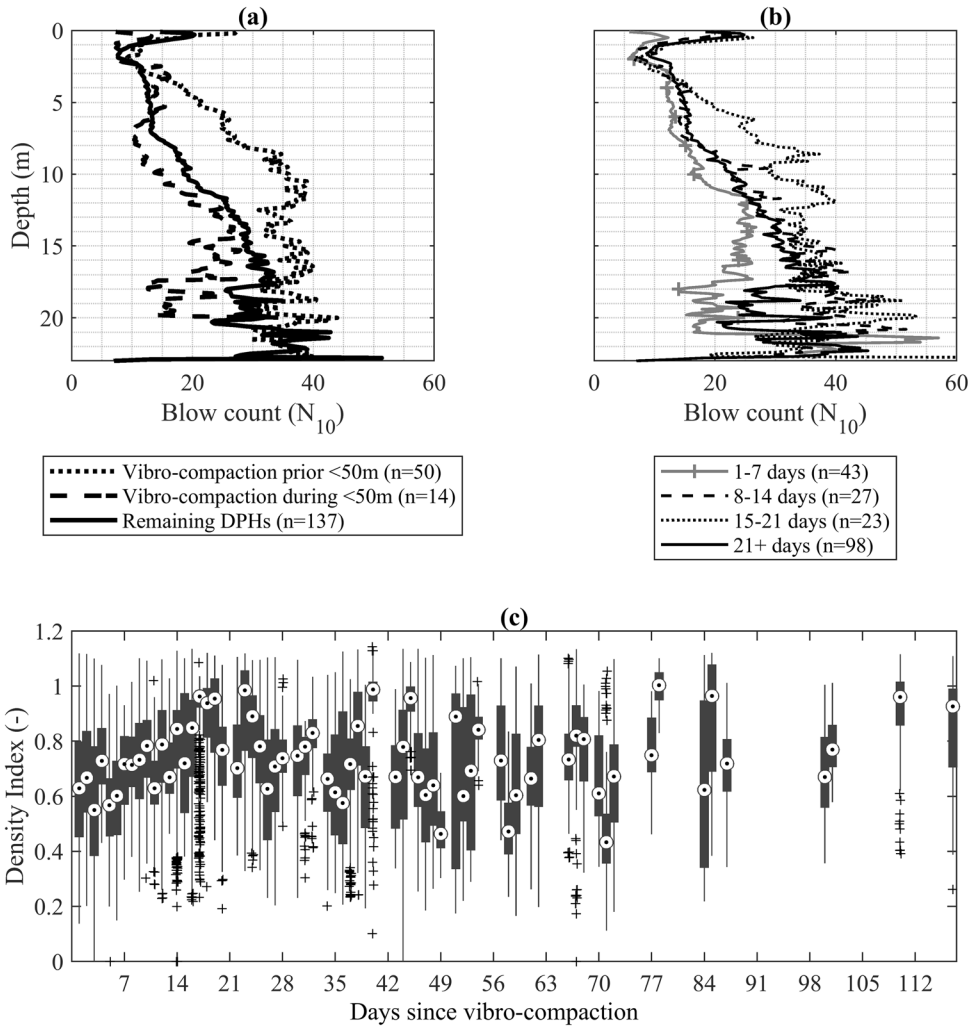

Fig. 5 **a** Effect of vibro-compaction within 50 m of the DPH tests, **b** influence of the time since compaction and **c** boxplot of the estimated density indices according to Cudmani [9] vs. the number of days since vibro-compaction; with the sample size *n*

travelling through the soil causing movement of the grains and allowing for an easier penetration of the DPH probe. Alternatively, vibro-compaction being carried out nearby, prior to performing the DPH tests (but not during) and in addition to the compaction point(s) adjacent to the test, resulted in a marked increase in the blow count, as compared to DPH tests where no (additional) vibro-compaction was carried out previously in the vicinity. This observation can be contrasted with the results in Fig. 6a, where the DPH tests corresponding to the 'Double Point' as illustrated in Fig. 6b record higher blow counts than at the 'Tripe Point.' One possible explanation for this observation is that extensive vibro-compaction causes a breakage of the grains in the immediate vicinity of the vibroprobe, thus causing a reduction in the shear strength and resistance to the penetration of the DPH probe. Another explanation is the nature of compacted coarse grained soil to dilate as a consequence of large shearing. To assess this effect, additional analysis of the test compaction results would need to be undertaken, including additional DPH testing at varying distances from the compaction points.

Based on the assumption of a homogenous fill material it is expected that the amount of fill material added during the vibro-compaction process, quantified by the bucket count would be representative of the amount of compaction experienced by the soil grains in the vicinity of the vibro-compaction. This hypothesis is explored by comparing the average density index with the adjacent average amount of fill material added at the compaction points as seen in Fig. 7a. Here no correlation (a negative correlation could also be argued) between the achieved density index and the amount of material added at the compaction point(s) can be observed, indicating a variation in the shear strength of the material—which governs the resistance to penetration from the DPH probe. From Fig. 7b it is evident that there is a no correlation between the amount of additional fill material

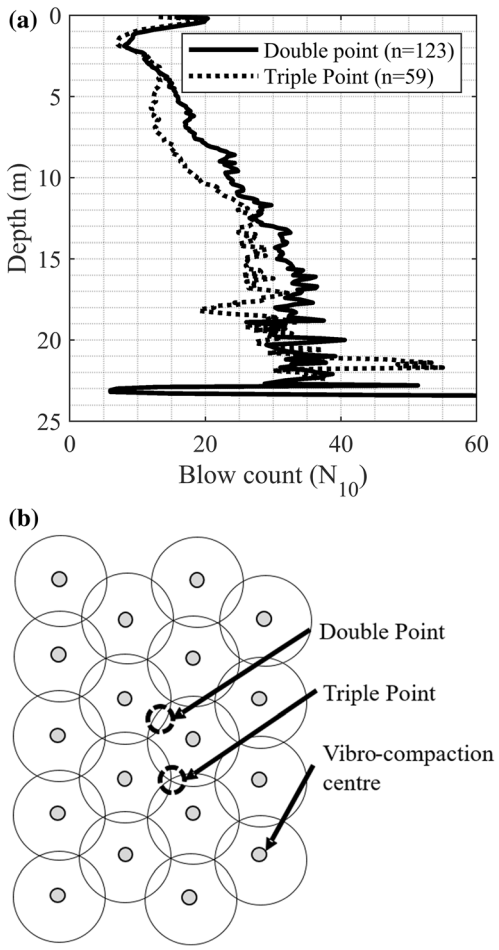

Fig. 6 **a** Influence of the DPH test location on the blow counts and **b** schematical description of the testing points

fed into the subsided compaction hole and the date of the vibro-compaction, indicating no dependence on the sequence of the vibro-compaction. Following from Fig. 7c there appears to be an incidental relationship between the amount of volume added during the vibro-compaction and when the DPH tests was carried out, possibly indicating that the areas tested with the DPH test first corresponded to an area with a naturally higher variability—which also appears to correlate with Fig. 7b where the vibro-compaction undertaken during Sep–Oct 2016 showed a greater variability.

The spatial correlation of the density index along the length of the dam (which in turn would be influenced by the variability of the source material) can be assessed from Fig. 8a, where there appears to be a slight negative trend. The amount of fill material added during the vibro-compaction process, quantified by the bucket counts, is also evaluated in Fig. 8b. Here also no significant trend was observed. In both plots an area at approximately Station 1+120 to 1+250, can be seen where the amount of fill material added is quite high and the density index appears to vary significantly. From Station 1+250 to 1+400, the fill material appears to be consistent, albeit with less scatter than Station 1+000 to 1+120 (based on the bucket counts). It can be concluded that this variability in the volume of material added is more likely to be the result of a spatial variability of the source material—e.g., more angular fill material leading to a greater propensity of the grains to break during the vibro-compaction than of varying compaction methods. In order to maintain a conservative estimate of the spatial variability of the dam fill and due to the absence of a physical justification, it was decided not to detrend the data to account for any linear correlation—which would have the effect of reducing the variability and increasing the correlation length.

In summary, the interpreted DPH test data were filtered, removing: (1) tests conducted 1–14 days after compaction at the adjacent compaction point; (2) tests conducted while vibro-compaction was being performed in the vicinity; and (3) tests conducted where additional vibro-compaction was undertaken with in the vicinity (in addition to the adjacent compaction point).

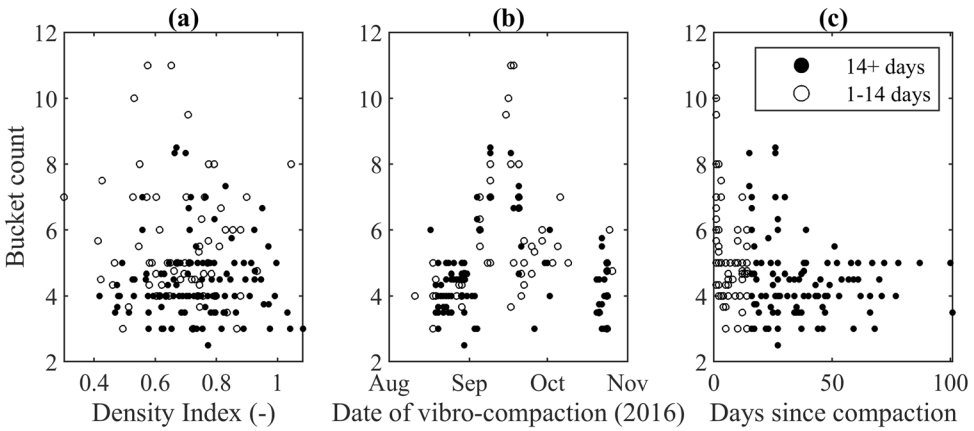

Fig. 7 Bucket count vs. **a** density index, **b** date of vibro-compaction (at compaction point) and **c** days since compaction (DPH test)

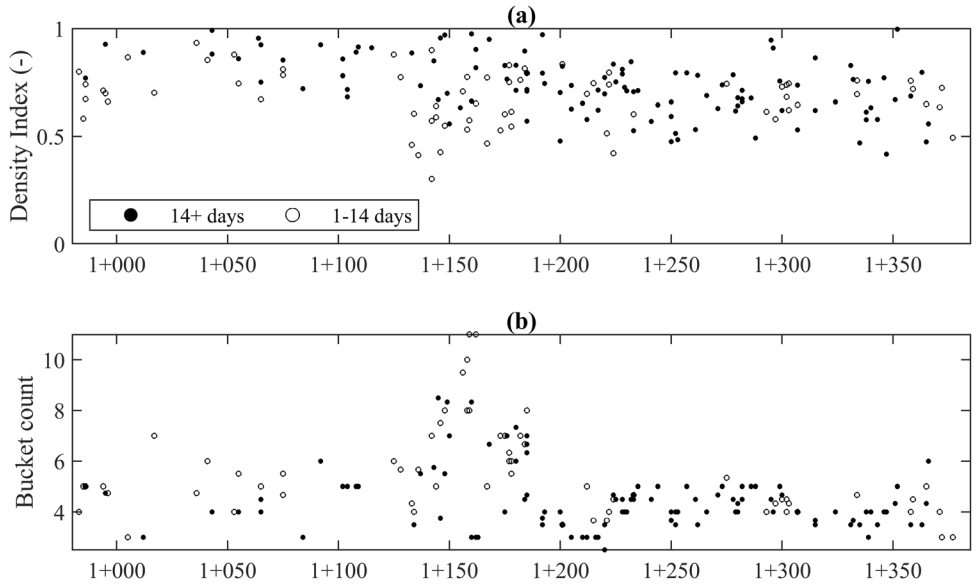

Fig. 8 **a** Variation in the estimated density index over the dike and **b** corresponding bucket counts, accounting for number of days since compaction, after which the DPH test was performed

2 Spatial correlation

The typically observed increasing dissimilarity of soil samples with increasing separation distance is caused by the inherent natural variability of natural materials, a phenomena that occurs even in relatively homogenous layers, and has been the focus of significant research (e.g., [10, 11, 31, 32, 38, 29 and 36]). The similarity of soils from two locations can be expressed through the variogram $2\gamma(h)$, which describes the variance of the difference between two quantities with a separation distance s as

$$2\gamma(h) = \mathrm{var}[Z(s) - Z(s+h)] \tag{9}$$

where $Z(s)$ is the soil property of interest.

The interpreted and filtered DPH data are typically evaluated using the method of moments (MOM) estimator proposed by Matheron [23] of

$$\hat{\gamma}(h) = \frac{1}{2N(h)} \sum_{i=1}^{N(h)} [Z(s) - Z(s+h)]^2 \tag{10}$$

where $\hat{\gamma}(h)$ is the experimental semi-variogram, and $N(h)$ is the number of distinct sample pairs (or test locations) with lag distance h. According to Cressie [8] the estimator proposed by Matheron [23] can be significantly affected by the presence of outliers and as such the test data were also evaluated using the MOM estimator from Cressie and Hawkins [7] of

$$2\hat{\gamma}(h) = \frac{\left\{\frac{1}{N(h)} \sum_{i=1}^{N(h)} |Z(s) - Z(s+h)|^{\frac{1}{2}}\right\}^4}{(0.457 + 0.494/N(h))}. \tag{11}$$

These two estimators were compared, and it was found that the estimator from Cressie and Hawkins [7] was shown to reduce the scatter as well as the *nugget* variance.

The DPH data were evaluated considering for possible anisotropy of the spatial correlation by evaluating the horizontal separation between the DPH tests as $XY = \sqrt{(X_i - X_j)^2 + (Y_i - Y_j)^2}$ and the angle as $\varphi = \tan(XY/|\Delta Z|)$ where $\varphi = 0$ represents a separation in the vertical direction and $\varphi = \pi/2$ a separation in the horizontal direction. The experimental semi-variogram was fitted with an single model exponential variogram (nugget = 0.002, range = 5.6 m, sill = 0.048) with the results being depicted in Fig. 9. From Fig. 9 there appears to be a certain degree of anisotropy; this was however not considered for because of the possibility that external factors (such as time since vibro-compaction), which by definition are not present when considering the vertical direction, could be causing the increased variance.

3 Interpolation

The *Kriging* interpolation method was used to interpolate the DPH test data in order to obtain a continuous representation of the density of the core fill over the length of the dike. Kriging, also known as the best linear unbiased predictor—best in that the prediction variance is minimized and unbiased in that clusters of sample points do not dominate the prediction, uses the semi-variogram to calculate the weights λ_i from samples (or observations) x_i for

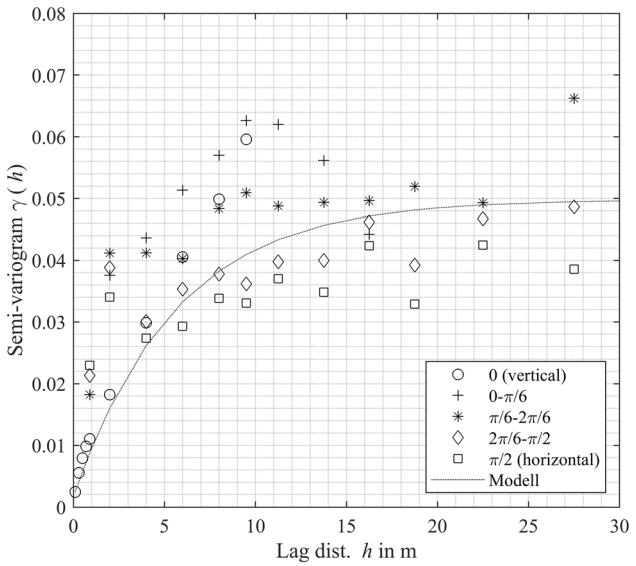

Fig. 9 Experimental semi-variogram binned into various separation angles and the fitted exponential model

the interpolation and can be performed either punctually or as a block average.

Many variations of Kriging exist; however, for the interpolation of the DPH test results *Ordinary Kriging* will be used, which assumes stationarity of the data, i.e.,

$$E[Z(\boldsymbol{x}) - Z^*(\boldsymbol{x})] = 0 \tag{12}$$

where $Z^*(\boldsymbol{x})$ is the estimate of the random process $Z(\boldsymbol{x})$. The theory can be summarized as follows: A value Z can be predicted at a location x_0 from the observation points as

$$\hat{Z}(x_0) = \sum_{i=1}^{N} \boldsymbol{\lambda}_i z(\boldsymbol{x}_i) \tag{13}$$

with the condition that

$$\sum_{i=1}^{N} \lambda_i = 1 \tag{14}$$

The weights $\boldsymbol{\lambda}$ in vector form are determined through the relationship

$$A\lambda = \boldsymbol{b} \tag{15}$$

where $\boldsymbol{A}$ is the matrix of semi-variograms between the sample points i and j and $\boldsymbol{b}$ is the vector of semi-variograms between the sample points i and the interpolation point. The variance of the Kriging estimate can be calculated as

$$\hat{\sigma}^2_{x_0} = \boldsymbol{b}^{\boldsymbol{T}}\boldsymbol{\lambda} \tag{16}$$

and the lower bound as

$$\hat{Z}_{LB}(x_0)\hat{\sigma}^2_{x_0} = \hat{Z}_{LB}(x_0) - 1.96\hat{\sigma}_{x_0} \tag{17}$$

based on the 95% confidence interval and assuming a normal distribution of the interpolated values. The interpolation points are chosen such as to be along the centerline of the dike core based on a grid with points every 2 m (h orizontally) and 0.5 m (vertically) along the length and depth of the dam, respectively.

The interpolated density indexes at the interpolation points according to the relationship proposed by Cudmani [9] can be seen in Fig. 10, wherein (a) the interpolated density index is shown using only the DPH tests subject to the three above-mentioned criterion (n = 83). In the figure blue corresponds to the theoretical maximum density index of 1, green corresponds to the target density index of 0.7, and red corresponds to a density index of 0.4. In Fig. 10b the interpolated density index is shown, this time considering all the DPH tests over 14 days of age (n = 123), in (c) a lower bound of the Kriging estimate [see Eq. (17)] is shown and in (d) the Kriging variance. From this plot it is evident that according to (a) the very large majority of the dike has a density index far exceeding the target. Isolated areas do appear to have a lower target density such as Station 1+150 to 1+200 (corresponding to the large bucket counts noted previously) and at approx. Station 1+350. It can also be seen in a comparison of (a) and (b) that excluding DPH tests carried out while vibro-compaction is being carried out in the area has a large impact in the interpolation of the density index, e.g., large areas at Station 1+000 to 1+050 are identified as not being adequately vibro-compacted. Due to the significantly high Kriging variance (due to relatively small correlation length and relative sparcity of the data) and spatial scattering of DPH tests the lower bound estimate is very low, with only few areas having a density index of higher than a loose to medium dense state. In summary, isolated pockets of areas with a density index lower than the specification can be identified (so called "soft spots"); however, it is important to note that these areas do not generally extend to the entire depth of the dam fill. Additionally, care should be taken in using the Kriging estimate in areas where there is a high variances, as there are insufficient data to provide an accurate estimation—as such consideration should be given to the lower bound estimate, which as has been shown here, can be excessively conservative.

4 Assessment of the compaction effort

To assess the adequacy of the compaction, (1) the presence of areas with an apparent lower density must be ascertained, and (2) it must be evaluated whether this lower density is the result of a spatial variability of the shear strength of the fill material. For (1) the authors suggest a

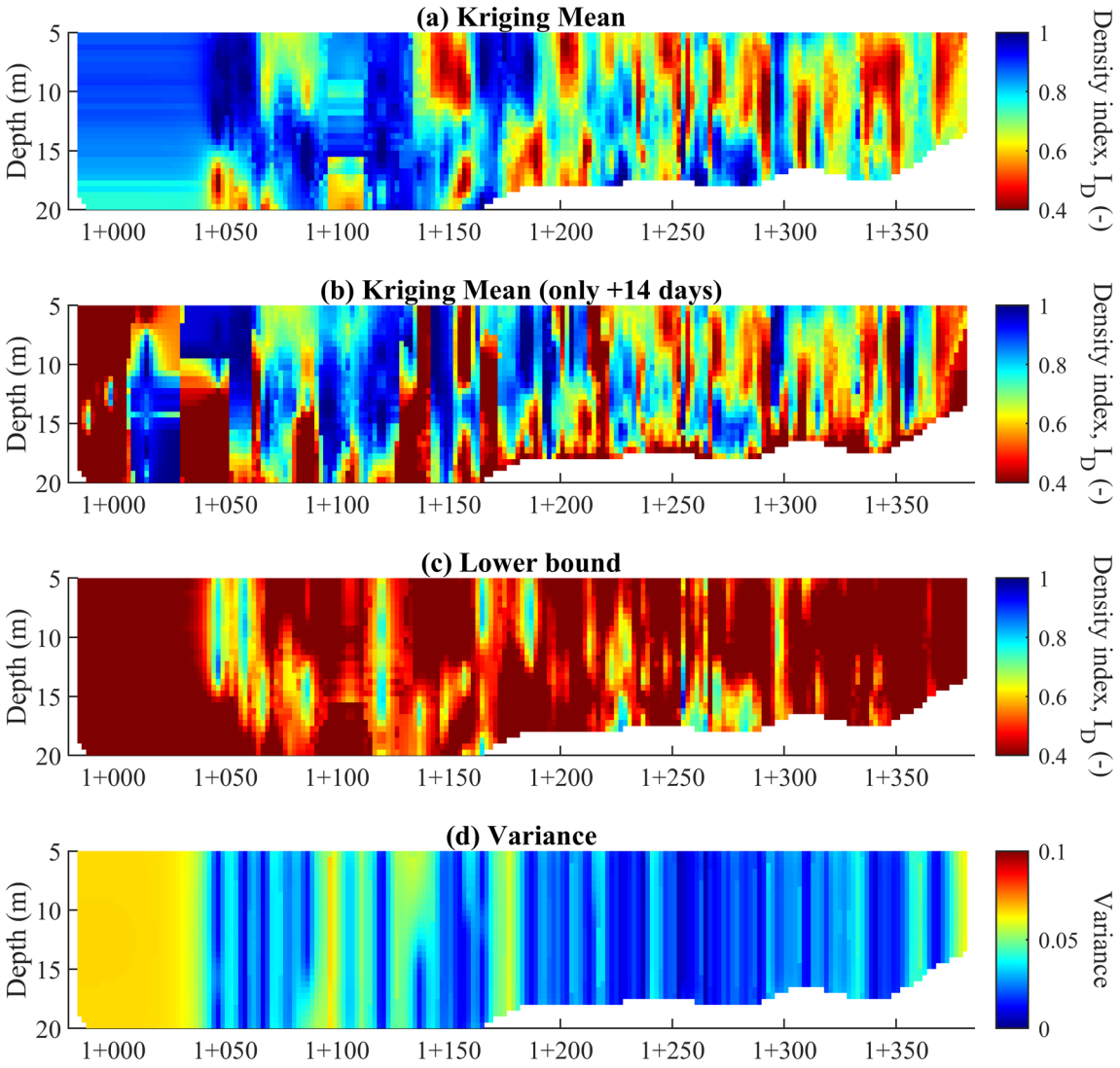

Fig. 10 Interpolated Kriging mean of **a** selected DPH tests and **b** all tests DPH tests 14 + days after compaction, **c** lower bound estimate of the kriging mean and **d** Kriging variance [in **a**, **b** and **c** areas in shades of yellow and red correspond to a density index lower than the target]

comparison of the success of the compaction based on the Kriging estimate of the density index. From the presented results in Fig. 10a one can see that there are several isolated areas along the length of the dike which have been identified as probably having a density index lower than the target (e.g., between Station 1+150 and Station 1+350).

For (2), without knowledge of the state of the fill material prior to compaction it is difficult to make a distinction between the natural variability of the soil and inadequate compaction. In this case, the authors recommend a procedure involving averaging the interpolated density indexes using a moving window based on the scale of fluctuations δ (where $\delta = 2 \cdot r$, and r is equal to the identified range of 5.6 m ; see [32]) and comparing the averaged interpolated density index to a so called "expected density" The expected density is determined based on the premise that the density indexes in the vicinity of a given density index I_D^i (where i is a point on the interpolation grid) will, with increasing distance h from i, approach the mean density index of all the points $\overline{I}_D$, and that this similarity can be modelled using the variogram. Based on this relationship, the expected density index averaged over a distance R equal to δ, given I_D^i and $\overline{I}_D$, can be calculated as follows:

$$I_D^R = \frac{1}{R}\int_0^R f(I_D)\mathrm{d}h \tag{18}$$

where the function $f(I_D)$ is defined by:

$f(I_D) = \left(1 - \exp\left(-\frac{h}{r}\right)\right) \cdot \left(\overline{I}_D - I_D^i\right) + I_D^i$. (19).

Under the assumption that the presence of poor compaction can be defined by the average interpolated density

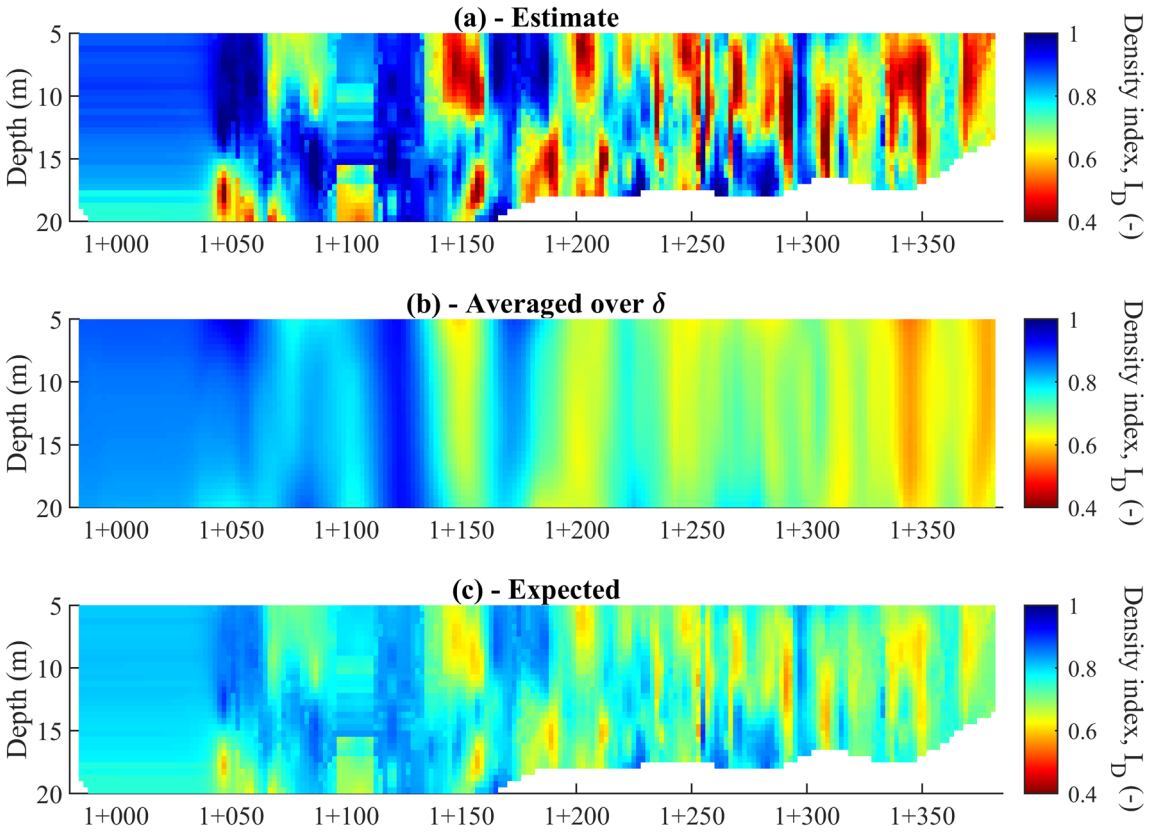

Fig. 11 **a** Kriging estimate, **b** average over a radius of δ and **c** expected average over δ

index within a moving window, over a certain distance R from i, defined a s $\widetilde{I}_{\mathrm{D}}^{R}$, being significantly lower than the above described, expected density index I_{D}^{R}. Thus, the points that most likely represent insufficient compaction can judged based on comparing $\widetilde{I}_{\mathrm{D}}^{R}$ and I_{D}^{R}. In Fig. 11 the Kriging estimate (a), the average interpolated density over δ (b) and the expected density index (c) based on Eq. (18) can be seen. Through a comparison between Fig. 11b and c one can see that there are areas where the moving window averaging results in a higher than expected I_{D}, as well as areas with a lower than expected I_{D}. This is to be expected, as the data cannot be described perfectly by the variogram. However it can be seen from a visual comparison that several areas, e.g., at Station 1+340, can be identified as having a lower averaged density index than expected and as such can be deemed to have inadequate compaction. The implication is that other areas, which appear to show an under-compaction (e.g., Station 1+150, due to their relatively limited size, can rather be attributed to the natural variability of the fill.

4.1 Conclusion

In summary, a method for interpreting the DPH tests within the core zone of Dike A21 within a statistical framework was presented; this involved determining the spatial correlation of the compacted fill material, interpolating the interpreted density index and using the spatial correlation to test for the presence of areas of insufficient compaction.

The normalization of the data to account for factors such as the mean pressure (depth) showed that the influence of the "aging" of the material, characterized as the time since vibro-densification, was found to be significant, where a linear increase in the interpreted density index was observed within the first 14 days. Thus, it is recommended that the control of densification shall be carried out at least two weeks after compaction. The increase penetration resistance with time was also observed in the recent DPH tests carried out on the Dike A418, which was constructed 10 years prior, where the resistances recorded were significantly larger than the values obtained for Dike A21. Thus, the penetration resistance obtained immediately after vibro-compaction is a conservative estimative, in comparison with the values expected sometime after construction, e.g., during the open pit mining. Additionally, it was shown through a comparison of the "double point" and "triple point" DPH tests that the over-compacted areas tended to perform worse, where it was hypothesized that this is due to breakage of the soil grains. As demonstrated through the normalization of the data and the analysis of the bucket

counts, the fluctuation in the in situ density is more likely to be caused by fluctuations in the homogeneity of the fill material.

Following the normalization of the data, the spatial correlation in the vertical and horizontal was determined, where a single exponential model was fitted to the experimental variogram. The correlation model was then used to interpolate the density indexes along the center-line of the dike and at various depths with Kriging. Some isolated areas with a density lower than the target were identified; however, it was shown that these areas of lower density could mainly be attributed to natural variability of the shear strength of the fill. A significant area was identified at Station 1+340 and possibly, also at Station 1+200, which could be interpreted as being under-compacted. It is the opinion of the authors that re-compaction is not however expected to improve the situation considerably. Rather, this can be counterproductive as the improvement of stiffness and strength due to aging may be erased by vibrations.

In conclusion, the natural variability of the material should be considered when assessing the performance of soil improvement works and a methodology was presented for performing this assessment objectively, should the quantity of data allow for it, and thereby the risk of an incorrect assessment of the compaction effort can be reduced. For large projects validation of the interpretation method (e.g., in the form of chamber calibration tests), considering both the natural and improved state, should ideally be performed which would further reduce the uncertainty.

Acknowledgements The authors wish to thank the Diavik Diamond Mines Inc. (DDMI) for supporting this research by providing the original DPH data and the relevant project information and for permitting their use in this publication. Finally, we would like to make clear that none of the parties involved in the planning, design and construction of the Diavik Diamond Mine project participated in the preparation of this research work.

Funding Open Access funding enabled and organized by Projekt DEAL.

Data availability Some or all data, models or code that supports the findings of this study is available from the corresponding author upon reasonable request. Some or all data, models or code generated or used during the study are proprietary or confidential in nature and may only be provided with restrictions. Some or all data, models or code used during the study were provided by a third party. Direct requests for these materials may be made to the provider as indicated in Acknowledgements.

References

1. Al-Naqshabandy MS, Bergman N, Larsson S (2012) Strength variability in lime-cement columns based on cone penetration test data. Proc Inst Civ Eng Ground Improv 165(1):15–30. https://doi.org/10.1680/grim.2012.165.1.15
2. Biedermann B (1984) Vergleichende Untersuchungen mit Sonden in Schluff. Forschungsberichte aus Bodenmechanik und Grundbau, Aachan
3. Bolton MD, Gui MW, Garnier J et al (1999) Centrifuge cone penetration tests in sand. Géotechnique 49(4):543–552. https://doi.org/10.1680/geot.1999.49.4.543
4. Bong T, Stuedlein AW (2017) Spatial variability of CPT parameters and silty fines in liquefiable beach sands. J Geotech Geoenviron Eng 143(12):4017093. https://doi.org/10.1061/(ASCE)GT.1943-5606.0001789
5. Butcher AP, McElmeel K, Powell JJM (1995) Dynamic probing and its use in clay soils. In: Advances in site investigation practice, pp 383–395
6. Charlie WA, Rwebyogo MFJ, Doehring DO (1992) Time-dependent cone penetration resistance due to blasting. J Geotech Eng 118(8):1200–1215. https://doi.org/10.1061/(ASCE)0733-9410(1992)118:8(1200)
7. Cressie N, Hawkins DM (1980) Robust estimation of the variogram: I. J Int Assoc Math Geol 12(2):115–125. https://doi.org/10.1007/BF01035243
8. Cressie NAC (2010) Statistics for spatial data. Wiley, New York
9. Cudmani R (2000) Statische, alternierende und dynamische Penetration in nichtbindigen Böden. PhD dissertation, Karlsruhe
10. Fenton GA (1999) Estimation for stochastic soil models. J Geotech Geoenviron Eng 125(6):470–485. https://doi.org/10.1061/(ASCE)1090-0241(1999)125:6(470)
11. Fenton GA (1999) Random field modeling of CPT data. J Geotech Geoenviron Eng 125(6):486–498. https://doi.org/10.1061/(ASCE)1090-0241(1999)125:6(486)
12. Ghafghazi M, DeJong JT, Wilson DW (2017) Evaluation of Becker penetration test interpretation methods for liquefaction assessment in gravelly soils. Can Geotech J 54(9):1272–1283. https://doi.org/10.1139/cgj-2016-0413
13. Jaky J (1948) Pressure in silos. In: Proceedings of the second international conference on soil mechanics and foundation engineering, Haarlem, Netherlands, pp 103–107
14. Jamiolkowski M, Ghionna VN, Lancellotta R, Pasqualini E (1988) New correlations of penetration tests for design practice. In: Proceedings of the 1st international symposium on penetration testing: ISOPT-1. AA Balkema, Rotterdam, vol 27, pp 263–296
15. Jamiolkowski M, Ladd CC, Germaine JT, Lancellotta R (1985) New developments in field and laboratory testing of soils. In: Proceedings of the eleventh international conference on soil mechanics and foundation engineering: San Francisco, 12–16 August 1985 = Comptes rendus du onzième Congrès Internationale de Mécanique des Sols et des Travaux de Fondations. Balkema, Rotterdam, pp 57–153
16. Karray M, Hussien MN (2018) Why is there a discrepancy in shear wave velocity—cone tip resistance ($V_s - q_c$) correlations' trends with respect to grain size? Can Geotech J 55(7):1041–1047. https://doi.org/10.1139/cgj-2017-0316

17. Khosravi A, Martinez A, DeJong JT (2020) Discrete element model (DEM) simulations of cone penetration test (CPT) measurements and soil classification. Can Geotech J 57(9):1369–1387. https://doi.org/10.1139/cgj-2019-0512
18. Kralik B (1984) Neuere Erkenntinisse bei Ramm- und Drucksondierungen. In: Petrasovits G (ed) Proceedings of the sixth budapest conference on soil mechanics and foundation engineering: Budapest, October 2–5, 1984. Akad. Kiadó, Budapest, pp 167–174
19. Li L, Huang J, Cassidy MJ, Kelly R (2014) Spatial variability of the soil at the Ballina national field test facility. Australian Geomechanics Journal 49(4):41–48.
20. Liu X, Liu E, Zhang D, Zhang G, Song B (2019) Study on strength criterion for frozen soil. Cold Reg Sci Technol 161:1–20. https://doi.org/10.1016/j.coldregions.2019.02.009
21. Liu QB, Lehane BM (2012) The influence of particle shape on the (centrifuge) cone penetration test (CPT) end resistance in uniformly graded granular soils. Géotechnique 62(11):973–984. https://doi.org/10.1680/geot.10.P.077
22. Mahler A, Szendefy J (2009) Estimation of CPT resistance based on DPH results. Periodica Polytechnica Civil Engineering 53(2):101. https://doi.org/10.3311/pp.ci.2009-2.06
23. Matheron G (1962) Traité de géostatistique appliquée. Technip, Paris
24. Melzer K-J (1968) Sondenuntersuchungen in sand. PhD dissertation, Aachen
25. Mitchell JK (2008) Aging of sand—a continuing enigma? In: Prakash S and University of Missouri-Rolla (eds) Sixth international conference on case histories in geotechnical engineering and symposium in honor of Professor James K. Mitchell, August 11–16, 2008, Arlington, Virginia. University of Missouri-Rolla, Rolla
26. Mitchell JK, Soga K (2005) Fundamentals of soil behavior, 3rd edn. Wiley, Hoboken
27. Mitchell JK, Solymar ZV (1984) Time-dependent strength gain in freshly deposited or densified sand. J Geotech Eng 110(11):1559–1576. https://doi.org/10.1061/(ASCE)0733-9410(1984)110:11(1559)
28. Pan Y, Liu Y, Tyagi A, Lee F-H, Li D-Q (2021) Model-independent strength-reduction factor for effect of spatial variability on tunnel with improved soil surrounds. Géotechnique 71(5):406–422. https://doi.org/10.1680/jgeot.19.P.056
29. Phoon K, Nadim F, Uzielli M, Lacasse S (2006) Soil variability analysis for geotechnical practice. In: Phoon K, Hight D, Leroueil S, Tan T (eds) Characterisation and engineering properties of natural soils. Taylor & Francis, Milton Park
30. Phoon K-K, Ching J (2015) Risk and reliability in geotechnical engineering. Taylor and Francis, Hoboken
31. Phoon K-K, Kulhawy FH (1999) Characterization of geotechnical variability. Can Geotech J 36(4):612–624. https://doi.org/10.1139/t99-038
32. Phoon K-K, Quek S-T, An P (2003) Identification of statistically homogeneous soil layers using modified Bartlett statistics. J Geotech Geoenviron Eng 129(7):649–659. https://doi.org/10.1061/(ASCE)1090-0241(2003)129:7(649)
33. Renzi R, Corte JF, Bagge G, Gui M, Laue J (1994) Cone penetration tests in the centrifuge: experience of five laboratories. In: Leung CF, Lee FH (eds) Centrifuge 94: proceedings of the international conference centrifuge 94, Singapore, 31 August–2 September 1994. Balkema, Rotterdam, pp 77–82
34. Slocombe BC, Bell AL, Baez JI (2000) The densification of granular soils using vibro methods. Géotechnique 50(6):715–725. https://doi.org/10.1680/geot.2000.50.6.715
35. Solymar ZV, Reed DJ (1986) A comparison of foundation compaction techniques. Can Geotech J 23(3):271–280. https://doi.org/10.1139/t86-040
36. Stuedlein AW, Kramer SL, Arduino P, Holtz RD (2012) Geotechnical characterization and random field modeling of desiccated clay. J Geotech Geoenviron Eng 138(11):1301–1313. https://doi.org/10.1061/(ASCE)GT.1943-5606.0000723
37. Uzielli M, Vannucchi G, Phoon KK (2005) Random field characterisation of stress-nomalised cone penetration testing parameters. Géotechnique 55(1):3–20. https://doi.org/10.1680/geot.2005.55.1.3
38. Vanmarcke E (1983) Random fields: analysis and synthesis. MIT Press, Cambridge
39. Vanmarcke EH (1977) Probabilistic modeling of soil profiles. J Geotech Eng Div 103(11):1227–1246
40. Zhao HF, Zhang LM, Xu Y, Chang DS (2013) Variability of geotechnical properties of a fresh landslide soil deposit. Eng Geol 166(3):1–10. https://doi.org/10.1016/j.enggeo.2013.08.006
41. BGC Engineering (2014) Diavik Diamond Mines Inc., Dike A21 Design Update, dated 28.11.2018